Reaction and diffusion at the reservoir/shale interface during CO_2 storage

Victor N. Balashov[1], Susan L. Brantley[1], George D. Guthrie[2], Christina L. Lopano[2] and J. Alexandra Hakala[2]

[1]Earth and Environmental Systems Institute, 2217 EES Building, Pennsylvania State University, University Park, PA 16802

[2] U.S. Department of Energy, National Energy and Technology Laboratory, 626 Cochrans Mill Road, Pittsburgh, PA 15236

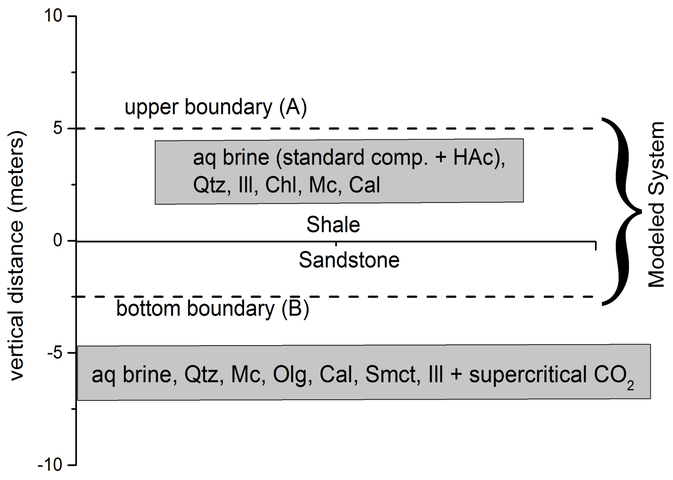

Figure 1. The modeled contact sandstone/shale.

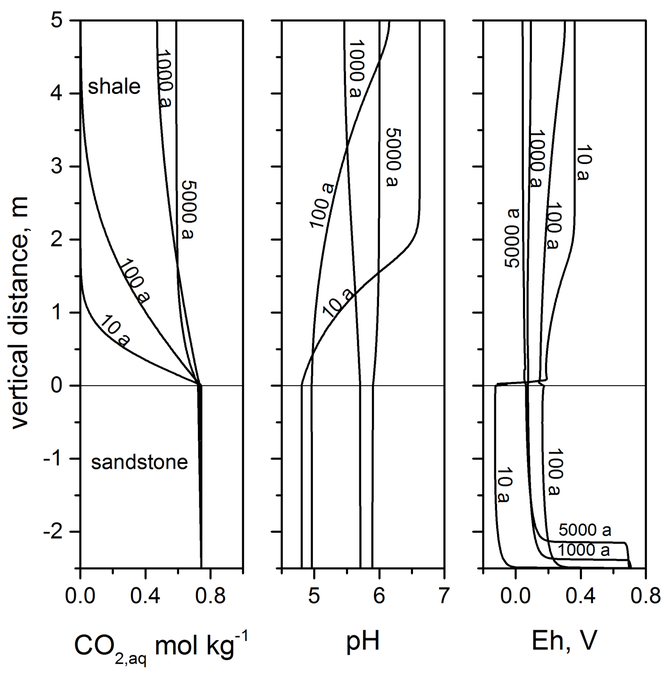

Figure 2. Profiles showing distributions of aqueous CO_2, pH, and Eh plotted versus depth across the shale (upper) - sandstone (lower) contact. Curves are labelled with the time after beginning of the CO_2 diffusion into the sandstone.

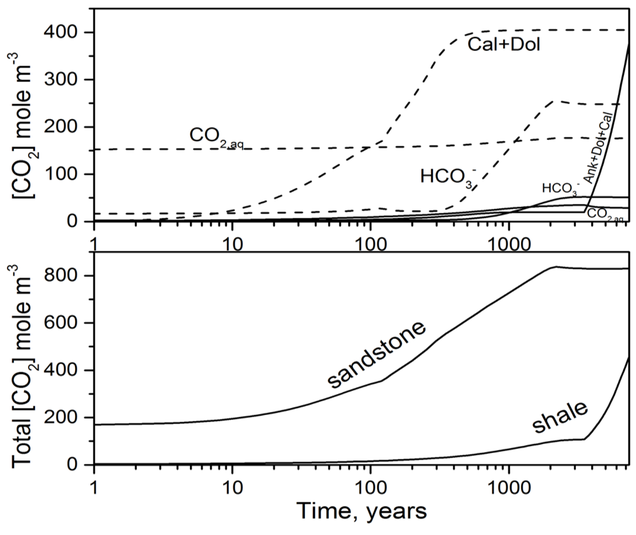

Figure 3. The average CO_2 accumulated per m^3 in a 2.5 m layer in the sandstone and a 5 m layer in the shale plotted versus time. The dashed and solid lines correspond to sandstone and shale layers, respectively. Top graph: the lines show the dissolution of molecular CO_2 into the brine, the CO_2 dissolution with conversion into HCO_3^-, and the CO_2 trapped due to carbonate (ankerite, dolomite, calcite) precipitation, as indicated. Bottom graph: the lines correspond to the total summed accumulation of CO2 trapped in sandstone and shale by the three mechanisms. The termination time (7416 a) corresponds to the complete sealing of the shale porosity at the ss/sh interface.

ABSTRACT

Reactive diffusion calculations were run to simulate storage of supercritical CO2 in a hypothetical reservoir at the sandstone/shale (ss/sh) interface at 348.15 K and 30 MPa. The shale functioned up to 2000 years as a low-permeable barrier, and the chemical reactions mostly occurred in the sandstone. In the period of 4000–7500 years, the replacement of Mg-Fe chlorite by dolomite, ankerite and illite at the ss/sh interface led to closure of the porosity at the interface, sealing the reservoir. We also ran sensitivity tests to understand the effect of varying the kinetic constants for the feldspars and clay minerals. The increase in the kaolinite kinetic constant by 0.5 and 1 logarithmic units resulted in faster sealing of sandstone reservoir because of chlorite carbonation at ss/sh contact by 650 and 107 years, respectively. The general reaction schemes were analyzed involving organic compounds in sedimentary basins from kerogen to carboxylic and carbonic acids in pore brines. The computations were carried out for extended ss/sh interface model with the initial presence of acetic acid in the shale pore brine at molalities of 0.01, 0.005 and 0.001. The reaction CH3COOH+2H2O=2CO2+4H2 led to the formation of redox front propagated into sandstone. The increase in Fe(II) activity in pore solution at ss/sh interface induced the earlier start of chlorite carbonation reaction in shale. The porosity closure times rank from 350 years at initial acetic acid molality of 0.01 to 5800 years at acid molality of 0.001.

METHOD

To solve the full reaction – diffusion problem of interaction of supercritical CO2 in brine-filled sandstone capped by shale, the program, MK76, was utilized. The heterogeneous system consisted of one aqueous and several mineral phases including supercritical (SC) CO_2. MK76 forms and solves the system of differential equations in partial derivatives for reactive diffusion mass transfer (Balashov et al., 2013, 2015).

THERMODYNAMICS

The thermo data were compiled from published data (Holland and Powell, 1998; Holland and Powell, 2011) for the minerals, and from Supcrt92 (Johnson et al., 1992) (Pokrovskii and Helgeson, 1995) for the aqueous species. The smectite and chlorite Gibbs free energies of formation from elements was calculated through the sum of polyhedral contributions by a published method (Chermak and Rimstidt, 1989; Chermak and Rimstidt, 1990).

KINETICS

The rate laws describing mineral dissolution/precipitation were formulated following a published approach (Brantley, 2008; Köhler et al., 2003; Lowson et al., 2007; Lowson et al., 2005; Marini, 2007; Palandri and Kharaka, 2004).

ORGANIC ACIDS IN SHALE BRINE

The main carboxylic acids in brine are acetic and propionic acids (Seewald, 2001). The concentration of acetic acid is 5-10 times greater than propionic. On the basis of geochemical data and thermodynamic calculations (Shock, 1988; Helgeson et al., 1993) we have assumed the equilibrium in pore fluid CH3COOH+2H2O=2CO2+4H2 . This assumption corresponds to the much faster oxidation of acid in comparison with decarboxylation (McCollom and Seewald, 2003).

CONCLUSIONS

Our modeling of reactive transport in the contact between a CO_2 storage reservoir (sandstone) and caprock (shale) has shown that the extent of C sequestration is highly sensitivite to the kinetic constants describing reactions of the clay minerals (kaolinite and illite) and to the carboxylic acids content in the shale. Chlorite plays a particularly key role in the development of the reactive zone in the shale. In most cases, the chlorite transforms due to carbonation into ankerite, dolomite and illite (or kaolinite), leading to autosealing of the ss/sh contact. An increase in the kinetic constants describing the clay minerals results in a remarkable decrease in the autosealing times. When these constants are smaller, the autosealing time increases. The relatively small increase of the carboxylic acids content in the shale leads to more reducing environment and results in the porosity sealing higher rate. This modeling is useful toward increasing our understanding of the sustainability of CO_2 storage in sandstone reservoirs beneath shale caprock.

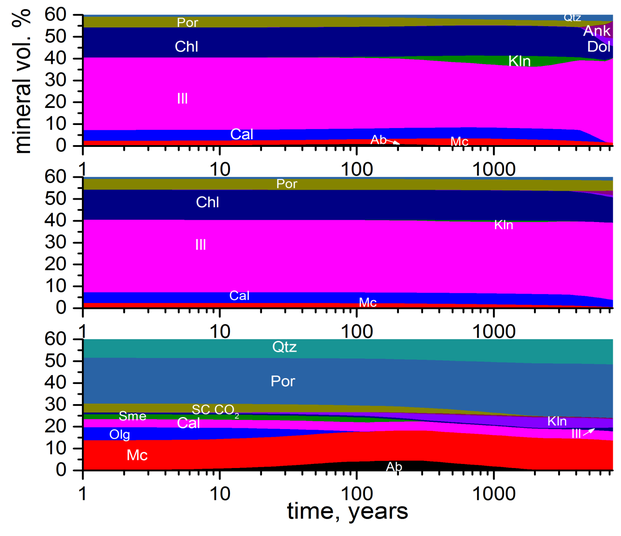

Figure 4. The evolution of the average mineral volume fraction of different minerals in shale at the sandstone/shale interface (top), inside the shale for the entire 0 to 1 m sub-layer above the interface (middle), and in the sandstone for the entire 0 - 2.5 m layer of sandstone (bottom).

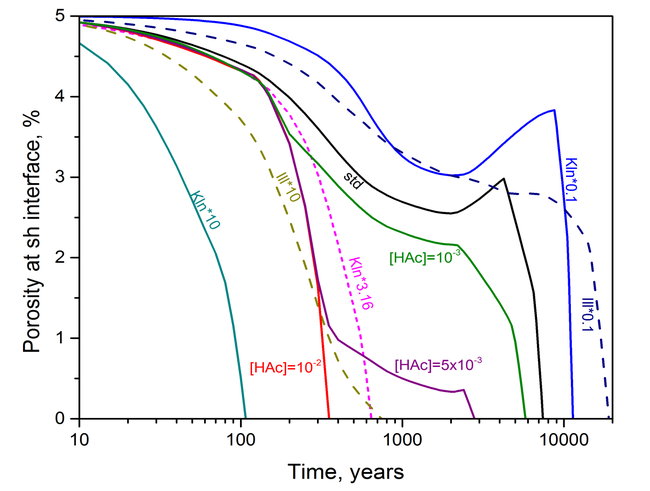

Figure 5. Curves describing the closure of porosity as a function of time for calculations assuming varying mineral kinetic constants and initial HAc molality in shale pore brine as indicated.

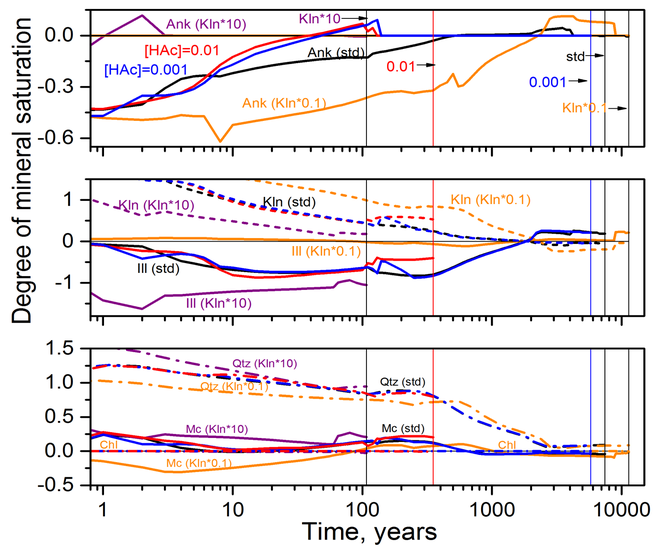

Figure 6. The evolution of ankerite saturation is represented in the top figure for a simulation where the kaolinite kinetic constant was set i) 10 times greater than the standard published constant, ii) equal to the standard kinetic constant, iii) 10 times less than the standard constant. The effects of acetic acid content in the shale brine are represented by red (0.01 mol/kg) and blue (0.001 mol/kg) curves. Saturation with respect to calcite and dolomite are indicated by the zero line. The saturation time for kaolinite (dash) and illite (solid) are plotted in the middle figure. The saturation time for quartz (long dash – dot), microcline (solid), and chlorite (dash-dot) are plotted in the bottom figure. The vertical lines show the termination times for different values of the kaolinite kinetic constant and acetic acid molalities, i.e., from left to right: 107.5, 7416, and 11,370 years for kaolinite constants equal to 10, 1, or 0.1 times the published value; 350 and 5800 years for 0.01 and 0.001 mol/kg, respectively.

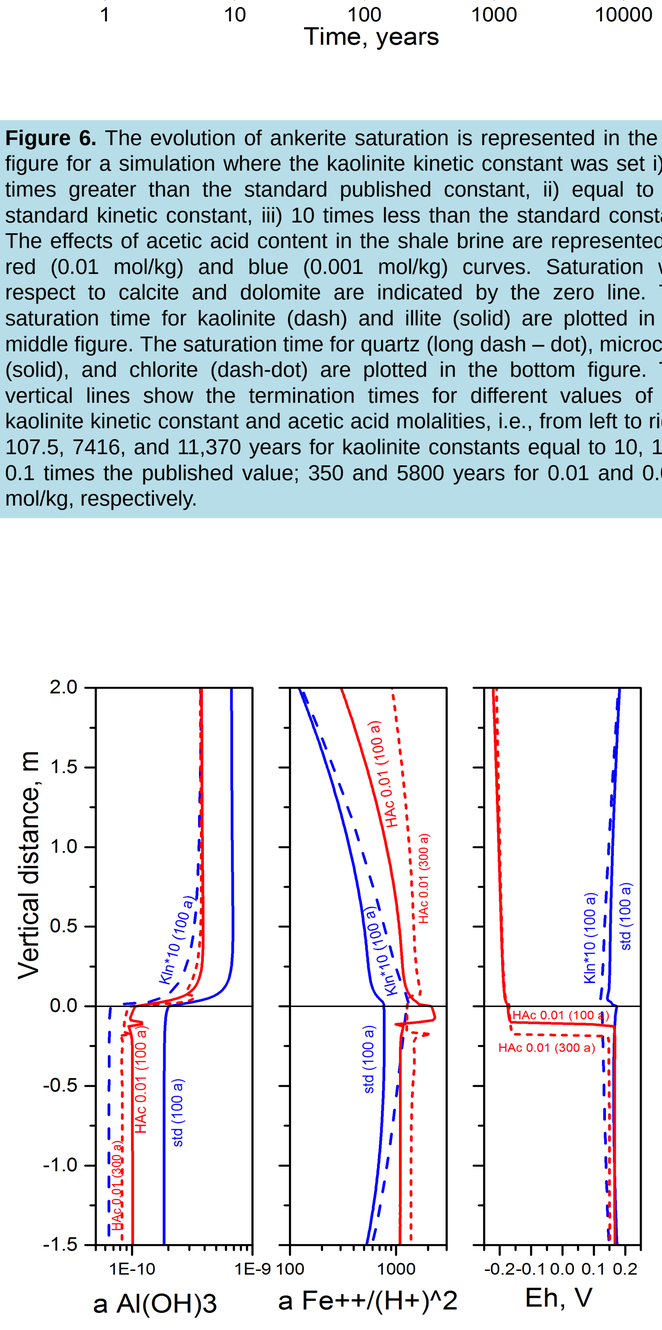

Figure 7. The activities of primary dissolved aqueous species ($a_{Al(OH)3}$ and a_{Fe++} a_{H+}^{-2}) and Eh plotted versus vertical distance across the ss/sh contact (plotted at 100 and 300 years) for the case of a high value of the kaolinite kinetic constant (10 times the standard value) and for the case of the HAc molality 0.01 in comparison with the standard kinetic case. The decrease of alumina activity in the brine is accompanied by an increase in iron (II) activity in brine. The increase in iron (II) activity follows the decrease in Eh induced by acetic acid in shale brine.

ACKNOWLEDGMENTS

This effort was performed in support of the National Energy Technology Laboratory's research in Carbon Storage under RES contract DE_FE0004000 to SLB.

REFERENCES

Balashov, V. N., Guthrie, G. D., Hakala, J. A., Lopano, C. L., Rimstidt, J. D., and Brantley, S. L., 2013. *Applied Geochemistry* ***30***, 41 - 56.
Balashov, V. N., Guthrie, G. D., Lopano, C. L., Hakala, J. A., and Brantley, S. L., 2015. *Applied Geochemistry* ***31***, 119 – 131.
Brantley, S. L., 2008. In: Brantley, S. L., Kubicki, J. D., and White, A. F. Eds.), *Kinetics of water-rock interaction*. Springer.
Chermak, J. A. and Rimstidt, J. D., 1990. *American Mineralogist* **75**, 1376-1380.
Helgeson, H.C., Knox, A.M., Owens, C.E., and Shock, E.L., 1993, *Geochimica et Cosmochimica Acta* **57**, pp. 3295-3339.
Holland, T. J. B. and Powell, R., 2011. *Journal of Metamorphic Geology* **29**, 333 - 383.
Johnson, J. W., Oelkers, E. H., and Helgeson, H. C., 1992. *Comp. Geoscience* **18**, 899-947.
Köhler, S. J., Dufaud, F., and Oelkers, E. H., 2003. *Geochimica et Cosmochimica Acta* **67**, 3583-3594.
Lowson, R. T., Brown, P. L., Comarmond, M.-C. J., and Rajaratnam, G., 2007. *Geochimica et Cosmochimica Acta* **71**, 1431-1447.
McCollom, T.M. and Seewald, J.S., 2003. *Geochimica et Cosmochimica Acta* **67**, 3645-3664.
Palandri, J. L. and Kharaka, Y. K., 2004. U.S. Geological Survey, Menlo Park, California.
Seewald, J.S., 2001. *Geochimica et Cosmochimica Acta* **65**, 3779-3789.
Shock, E.L.,1988. Geology, v.16, p.886-890.